# EVALUATING DIFFERENTIAL GNSS TECHNIQUES FOR LANDING THE 1ST STAGE OF AN RLV – WITH A SKYDIVER EXPERIMENT

**Benjamin Braun [(1)], Markus Markgraf [(2)]**

*German Space Operations Center (GSOC), German Aerospace Center (DLR),*
*Münchener Str. 20, D-82234 Weßling*
*[(1)] +49 8153 / 28-2115, benjamin.braun@dlr.de*
*[(2)] +49 8153 / 28-3513, markus.markgraf@dlr.de*

## ABSTRACT

Reusable launch vehicles (RLV) in a vertical take-off vertical landing configuration require accurate measurements of the height above the ground during the final descent just before landing. It is proposed to use real-time kinematic positioning (RTK), which is a differential GNSS navigation method requiring a nearby reference GNSS antenna and receiver, to measure the rover's position with centimetre accuracy. The effects of the engine plume, vibration and multipath are challenging when using this carrier-phase based positioning method on an RLV. Especially the residual differential tropospheric error due to the rover and reference GNSS antennas being at different heights, primarily caused by humidity in the air, may hinder the successful fixing of the carrier phase ambiguities. To gain a better understanding of the RTK performance to be expected on a landing RLV, a skydiver experiment was conducted in April 2022. The skydiver was equipped with a rover GNSS receiver and a helmet with a GNSS antenna on top and an independent integrated navigation system serving as reference. The skydiver reached free fall velocities of up to 385 km/h, which is seen representative of the vertical velocity of an RLV. The paper describes the experiment procedure and the results of the experiment.

## 1 INTRODUCTION

As part of the trinational technology demonstration project CALLISTO ("Cooperative Action Leading to Launcher Innovation for Stage Toss-back Operations"), JAXA, CNES and DLR are jointly developing and maturing key technologies for a future European and Japanese reusable launch vehicle (RLV) [1][2][3]. The goal of the project is to build and fly a vertical take-off vertical landing (VTVL) launch vehicle demonstrator that returns to the launch site (RTLS) after its mission. Beginning in the second half of 2025, there will be ten different test flights within a period of six months with increasing apogee altitudes from several metres to up to 20 kilometres and increasingly complex trajectories from the former Diamant site at Europe's spaceport in French Guiana. The CALLISTO vehicle is 13.5 m tall, has a diameter of 1.1 m and weighs less than four tons at lift-off. An artistic illustration of the CALLISTO vehicle is shown in Figure 1.
The GNSS & Navigation Technology group at the German Space Operations Center (GSOC) is responsible for the development, qualification and operation of the GNSS subsystem that is part of the hybrid navigation system (HNS) used to estimate the vehicle's position, velocity and orientation [4]. Due to the high demands on the lateral position accuracy, especially during the boost phase immediately prior to landing, the pseudorange-based differential GNSS (DGNSS) method is used,

which enables horizontal position accuracies in the sub-metre range. The DGNSS system consists of the rover GNSS antenna and receiver aboard the vehicle, a reference station with a static GNSS antenna and receiver located near the landing pad and the uplink of correction messages from the reference station to the rover GNSS receiver via telecommand.
One of the goals of the CALLISTO project is to achieve the lowest possible propellant consumption for the RTLS phase of the mission in order to save as much usable take-off mass as possible for the payload. The landing phase of the CALLISTO vehicle is therefore designed in such a way that the RLV decelerates just enough by means of aerodynamic drag and engine thrust that the vertical velocity is close to zero at touchdown. The small remaining kinetic energy is absorbed by the spring-dampener systems of the landing legs. The chosen approach requires that the vehicle's height above the landing pad is known very accurately in the final flight phase. The closer the vehicle gets to the ground, the more accurate the height measurement has to be. This approach is chosen in favour of a more conservative approach in which the vehicle would decelerate to a small constant downward velocity of about 1 m/s already a few metres above the ground and then descend at this constant velocity until touchdown, but which would result in a higher fuel consumption. Table 1 lists the requirements on the position accuracy during the final landing phase of the CALLISTO vehicle. The critical requirement on the vertical position accuracy below 100 metres is marked red.

Table 1: Requirements on the position accuracy during the final landing phase

| **Flight phase** | **Position [m] (at 99% probability)** | | **Required differential GNSS method** |
|---|---|---|---|
| | Lateral | Vertical | |
| Beginning of landing boost | 1 | 10 | DGNSS |
| Below 100 m | 1 | 0.5 | RTK |

It was originally planned to measure the height above the ground in the final flight phase with radar altimeters integrated into the landing legs illustrated in Figure 1. However, preliminary studies have shown that radar faces many technical challenges. During the landing boost, the radar altimeters would be directly exposed to the engine plume and would experience significant heat stress. The hot gases of the engine plume may interfere with the transmission of the radar signal and thus falsify the measurement of the height above the ground. Especially at larger heights above the ground, the radar signal may be reflected by other adjacent structures, such as lightning rod towers, rather than the surface of the landing pad, resulting in biased measurements. At lower heights above the ground, dirt thrown up by the engine plume may cause false reflections, which may in turn result in noisy measurements and outliers that have to be reliably detected and isolated by the HNS. In the end, costs and risks of developing a reliable radar altimeter for CALLISTO overcoming the aforementioned technical challenges were deemed too high, and the original plans to use radar altimeters were discarded.
The GNSS & Navigation Technology group is therefore investigating whether the height can alternatively be measured reliably using the differential carrier phase-based real-time kinematic (RTK) positioning method. RTK with fixed ambiguities would provide centimetre-level measurement accuracy of the height once at least four carrier phase ambiguities have been successfully fixed to integer values. It is advantageous that no additional hardware and infrastructure is required for RTK besides the already existing DGNSS system. The accuracy of the pseudorange-based DGNSS navigation system is not sufficient to fulfil the vertical position accuracy requirement below 100 metres above the ground. However, more effort must be put into the design and placement of the rover GNSS antenna on the vehicle, because RTK is more demanding, for example, in terms of reducing the effect of multipath or exactly knowing the antenna phase centre, which in turn requires the careful calibration of the rover GNSS antenna. RTK provides the relative position vector between

Figure 1. Artistic illustration of the CALLISTO vehicle, a joint project of CNES, DLR and JAXA

the phase centres of the static reference GNSS antenna on ground and the rover GNSS antenna aboard the vehicle. To obtain the height measurement above the landing pad, which is eventually required by the guidance and control of the CALLISTO vehicle, the relative position vector between a unique reference point marked on the landing pad and the phase centre of the static reference GNSS antenna has to be surveyed with centimetre accuracy prior to the test flights, using RTK once again for the survey. This additional relative position vector has to be stored as a constant parameter in the HNS. The calculation of the height of the vehicle above the landing pad from the two relative position vectors is then straightforward. In order to reduce the effect of multipath, ideally several hours of measurements have to be collected for the survey.

There is limited experience on how RTK performs in such an application, and to the authors' knowledge, there are no reference applications in the literature. The principal functionality of RTK for the intended purpose has been proven by numerous GNSS signal simulator tests in the laboratory and theoretical analyses. However, not all effects can be realistically represented by the GNSS signal simulator tests. To gain an even better understanding of the RTK performance to be expected on an RLV, the question was asked whether the scenario of a landing RLV can be realistically replicated by a flight experiment? Simple ideas of small free-fall bodies dropped from a helicopter were quickly discarded due to the complexity of flight stabilization, parachute landing and recovery in favour of the appealing idea to outfitting a skydiver with a rover GNSS antenna and receiver. The skydiver is already equipped with a parachute and can land precisely on a predetermined target point, which greatly simplifies the recovery and reduces the experiment development time and costs. The skydiver's free fall phase prior to parachute deployment represents the final descent phase of an RLV quite realistically. However, one disadvantage is that the achievable downward velocity is slightly smaller than with a small free-fall body.

## 2 RTK FOR CONVENTIONAL QUASI-STATIONARY APPLICATIONS

RTK is a proven position estimation technique and is traditionally used for terrestrial applications such as land surveying, civil engineering, precision agriculture or unmanned aerial systems. These applications have in common that they are quasi-stationary and use more or less horizontally levelled geodetic-grade GNSS antennas, with the rover and reference GNSS antennas at approximately the same height. They use a dedicated reference station nearby or use the reference measurements of a virtual reference station (VRS) provided by a commercial or public RTK network correction service. Millimetre accuracy can be expected if the phase variations of the reference and rover GNSS antennas are calibrated and a dedicated reference station with short baseline length is used; centimetre accuracy

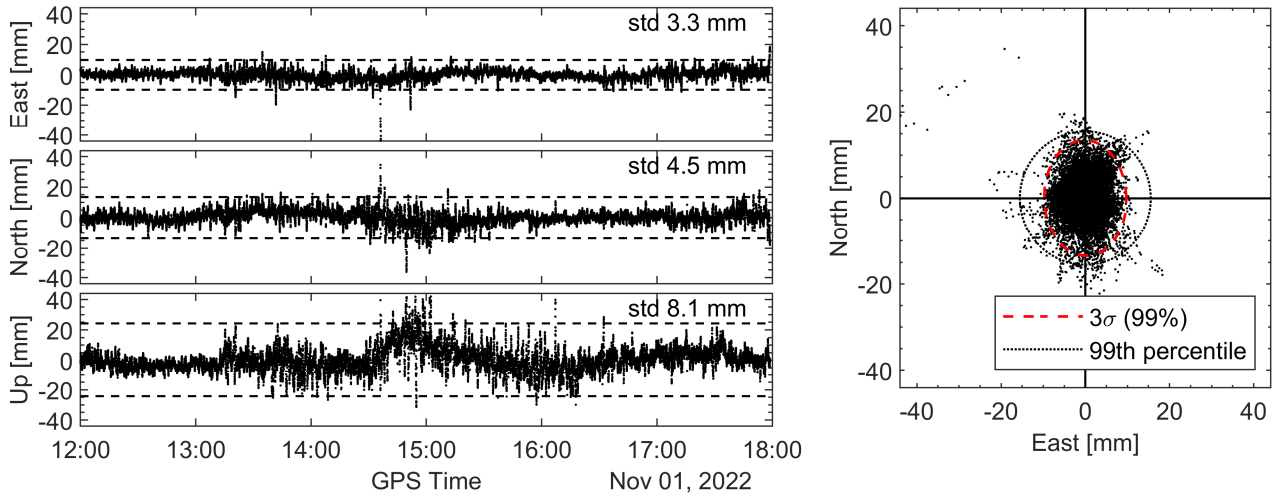


Figure 2. Position error of an exemplary RTK navigation solution between two static GNSS antennas located on the DLR site in Oberpfaffenhofen on November 1, 2022, using GPS and Galileo dual-frequency measurements

can be expected if the phase variations of the antennas are not calibrated and/or a VRS of an RTK network correction service is used.

To illustrate the accuracies achievable with RTK, a simple static test was performed with a stationary rover GNSS antenna on the roof of an office building on the DLR site at Oberpfaffenhofen. The IGS reference station OBE400DEU, which is also located on the site at a distance of about 400 metres from the rover GNSS antenna, served as reference station for this test. The rover GNSS antenna and receiver were geodetic-grade. A six-hour long period between 12 noon and 6pm (GPS time) on November 1, 2022 was analysed. For the RTK navigation solution, GPS and Galileo dual-frequency measurements were used, and the elevation mask was set to 15 deg. The position error in east, north and vertical directions is shown in Figure 2 on the left. The horizontal dashed lines are the 3σ standard deviations of the error over the six-hour period. As expected, the horizontal position error, with standard deviations of 3.3 mm and 4.5 mm, respectively, is approximately half the vertical position error, with a standard deviation of 8.1 mm. The distribution of the horizontal position error with the 3σ ellipse and the 99$^{th}$ percentile circle is shown on the right of Figure 2. It can be clearly seen that especially the vertical position error increases for a two-hour long period between 2:30pm and 4pm. This is due to multipath at the rover GNSS antenna because of an unfavourable satellite geometry during this phase. Nevertheless, the accuracy of the vertical position error meets the requirement for the height measurement during the landing phase of the CALLISTO vehicle. However, the example underlines the importance of taking precautions to reduce the influence of multipath at the rover and reference GNSS antennas.

## 3 TECHNICAL CHALLENGES OF USING RTK ON AN RLV

In contrast to the conventional quasi-stationary applications, RLV are characterized by high downward velocities and dynamics during the landing boost phase. The scenario is depicted in Figure 3. During the final 2,000 metres above the ground, only a few dozen seconds remain until touchdown, during which the ambiguities of a sufficient number of carrier phase measurements must be fixed to integer values in order to calculate a position solution with centimetre-level accuracy. Once an ambiguity has been successfully fixed, the signal has to be continuously tracked until landing. While in conventional quasi-stationary applications the rover and reference GNSS antennas are more or less at the same height, on an RLV the rover and reference GNSS antennas are initially at different heights

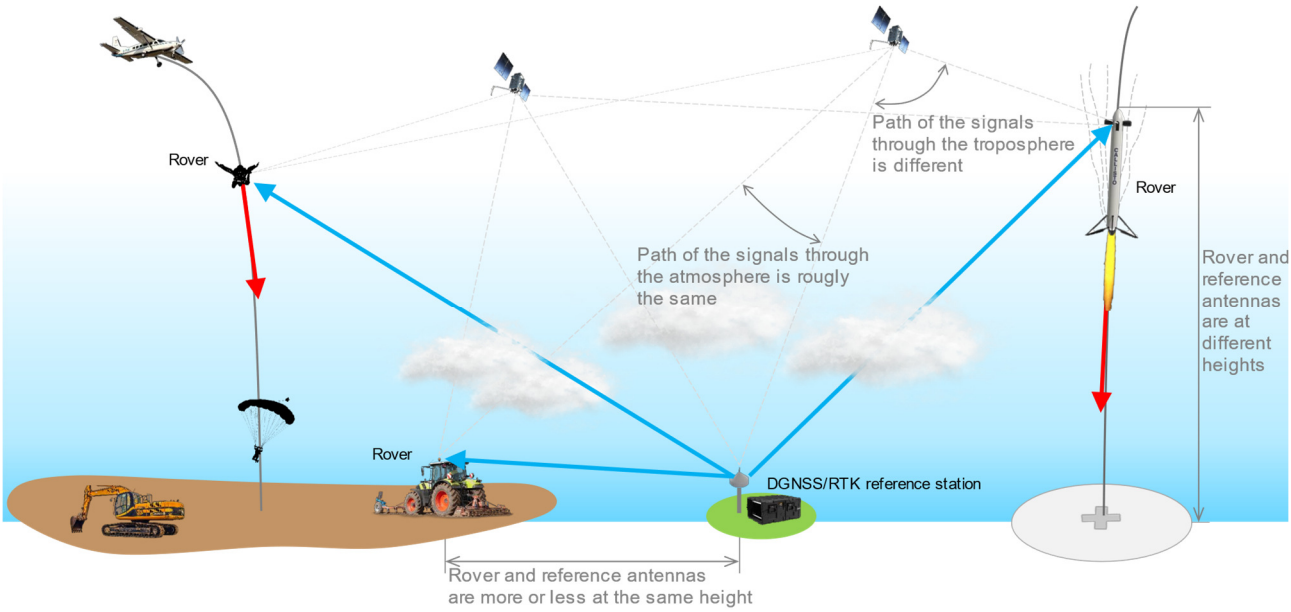


Figure 3. Using RTK on a landing RLV instead of for a conventional quasi-stationary application. The blue vectors are the relative position vectors to be estimated with centimetre-level accuracy.

when the RTK navigation solution is initialized and it is started to fix the ambiguities. Only then does the height difference between the rover and reference GNSS antennas decrease as the distance to the ground and thus the remaining flight time until touchdown decreases.

If the rover and reference GNSS antennas are at different heights, the path lengths of the GNSS signals through the troposphere received by the rover and reference GNSS antennas are different. The share of the tropospheric error that is not compensated by the applied troposphere model does not cancel out by differencing the measurements of the rover and reference GNSS receivers. Consequently, a residual differential tropospheric error remains on the single- or double-differenced pseudorange and carrier phase measurements. This residual differential tropospheric error, which may be in the range of centimetres to decimetres, may hinder the successful fixing of the carrier phase ambiguities. Since the residual differential tropospheric error depends primarily on the unmodelled humidity of the air, the effect varies regionally across the globe. Due to the very humid climate in the equatorial regions, the influence is especially large at Europe's spaceport in French Guiana and therefore needs to be particularly well understood and analysed for the application of RTK in the CALLISTO project.

Figure 4 shows curves of the air temperature, static pressure and relative humidity over height between 0 and 15 km which were measured by radiosondes released from the radiosonde station Altenstadt in Southern Germany during the two days of the skydiver experiment. It can be clearly seen that the temperature and static pressure do not vary very much in this 36-hour period. The characteristics of the dry air can be modelled very well by the commonly used troposphere models. The relative humidity, however, is subject to strong fluctuations. In the interesting range from 0 to 3 km above the ground, the relative humidity varies between 7.5% and 54%. The humidity in the air strongly depends on the current weather and cannot be well represented by globally valid troposphere models.

It is reassuring, however, that the residual differential tropospheric error decreases with decreasing height above the landing pad, consistent with the accuracy requirement for the height measurement, which is higher the closer the vehicle is to the ground.

Other challenges such as the effects of the engine plume passing the rover GNSS antenna, vibration from the engine, and multipath have to be overcome to provide accurate and reliable position estimates.

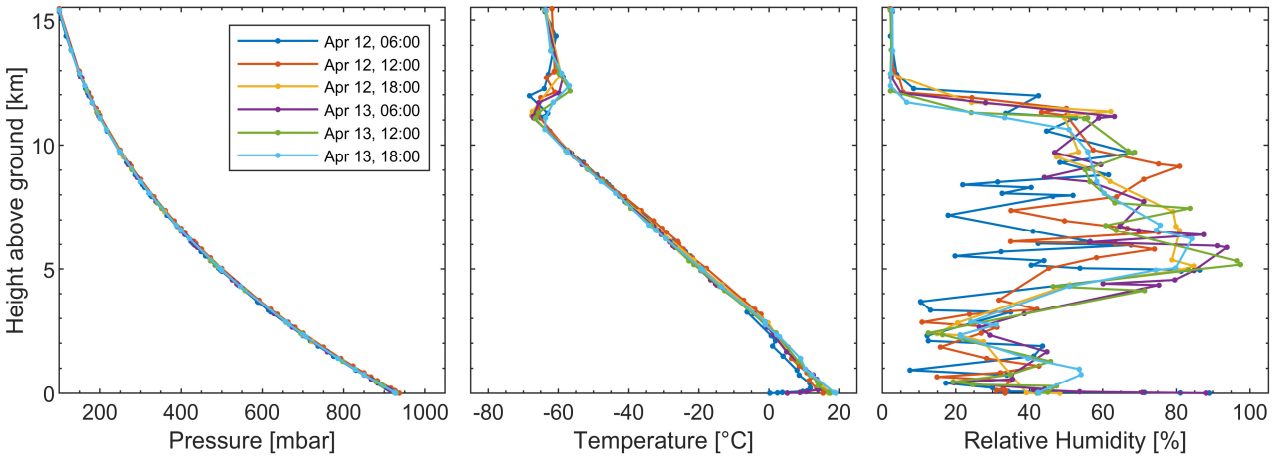

Figure 4. Radiosonde measurements on April 12–13, 2022 in Altenstadt, Germany (IGRA station code GMM00010954)

## 4 SKYDIVER EXPERIMENT

The skydiver experiment took place on April 12-13, 2022 at Leutkirch airfield in Southern Germany. A Cessna 208 aircraft served as carrier for the skydivers.

A special helmet was developed with a multi-frequency GNSS antenna, the attitude of which can be adjusted so that the antenna points upward, depending on the skydiver's planned flight pose. The geodetic-grade rover GNSS receiver, the model used in the CALLISTO project, was stowed in a fanny pack. In addition, an independent small integrated navigation system consisting of MEMS-based three-axis accelerometers, gyroscopes and magnetometers, as well as a barometer and another consumer-grade GNSS receiver, was installed on the helmet. It provided reference measurements for the post-processing analysis. The geodetic-grade rover GNSS receiver and the consumer-grade GNSS receiver of the integrated navigation system were connected to the same GNSS antenna on top of the helmet via a R/F signal splitter. For video footage, the helmet was also equipped with an action camera. The helmet with the instrumentation mounted on top of it is shown in Figure 5.

Additionally, a reference station, consisting of a geodetic-grade reference GNSS antenna and receiver, was set up near the airfield and was continuously operated to collect reference measurements during the two test flight days. All measurements of the flight and ground equipment were recorded during the flights and processed afterwards using a dedicated post-processing GNSS navigation software provided by the manufacturer of the geodetic-grade rover GNSS receiver. The post-processing software behaves exactly like the navigation engine of the geodetic-grade rover GNSS receiver. It obtained the recorded raw measurements of the rover and reference GNSS receivers and calculated a stand-alone, pseudorange-based DGNSS or carrier phase-based RTK navigation solution, depending on the availability and quality of the reference measurements at a dedicated epoch and the commanded positioning mode. Using this software not only simplified the experiment by eliminating the need for a real-time correction data uplink from the reference station to the rover GNSS receiver, but also made it easy to study the impact of different receiver settings, such as the troposphere model applied, by simply recomputing the navigation solution with different receiver settings. The manufacturer of the small integrated navigation system also provides a post-processing navigation software, with which a forward and backward smoothed navigation solution can be computed by fusing the accelerometer, gyroscope, magnetometer and DGNSS and RTK position and velocity measurements. For analysing the performance of the RTK navigation solution, the navigation

Figure 5. Helmet equipped with a multi-frequency GNSS antenna, integrated navigation system and data recording unit

solution of the geodetic-grade rover GNSS receiver was compared to the navigation solution of the independent integrated navigation system.

Basically, the rover GNSS receiver and the integrated navigation system were switched on still on the ground before take-off of the aircraft and only switched off again after the parachute landing. After turning on the sensors, the helmet was placed on a marked spot on the ground for a five-minute initialization phase. Within this phase, the rover GNSS receiver was able to acquire the signals from all visible GPS and Galileo satellites and to establish a stable stand-alone navigation solution, and the integrated navigation system estimated its initial orientation. After landing, the helmet was placed back on the same spot as at the beginning and left there for another five-minute recalibration phase before the sensors were switched off again. Because the rover GNSS receiver and the integrated navigation systems were operated from pre-take-off to post-landing, navigation solutions could be computed for the full cycle of take-off, climb, free fall and parachute landing.

Figure 6 illustrates the procedure of the test flights. First, the GNSS antenna on top of the helmet was adjusted to the skydiver's planned pose so that it pointed upwards as best as possible during the flight (a). After the five-minute initialization phase (b), the skydiver put on the helmet and stowed the rover GNSS receiver in the fanny bag. After a final flight safety check and a check, if the rover GNSS receiver and the integrated navigation system were working properly, the skydiver boarded the aircraft (c), the aircraft took off and the skydiver sat close to the radiotransparent door such that the rover GNSS antenna could still receive signals during the climb, even with the door closed (d). After the aircraft reached the drop altitude, the skydiver exited the aircraft and remained on a step outside the aircraft for a thirty-second reinitialization phase to allow the rover GNSS receiver to reacquire and stably track all GNSS signals (e). The proper functioning of the rover GNSS receiver was once again monitored by an engineer in the aircraft, who finally gave the skydiver clearance to fly. The skydiver jumped off, took the planned pose during the free fall (f) and finally opened the parachute at a height of about 1,200 metres above the ground and landed back on the airfield (g). The test flight ended with the five-minute recalibration phase (h).

(a) Adjustment of the GNSS antenna orientation

(b) Five-minute initialization phase after switch-on

(c) Boarding and final checks

(d) Climb

(e) Exit and thirty-second reinitialization phase

(f) Free fall

(g) Parachute landing

(h) Five-minute recalibration phase before switch-off

Figure 6. Test flight procedure

## 5 FLIGHT RESULTS

A total of ten flights each from about 4,000 metres above the ground were done. The skydiver took various poses, such as prone, stand-up or dive, reaching downward velocities of up to 385 km/h, which is nearly representative of the vertical velocity of the CALLISTO vehicle. Figure 7 illustrates the different poses of the ten flights. To get more confidence in the measurements and to examine the repeatability of the results, some of the flights were performed several times with the same pose. For example, the flight with prone pose, which is typical for skydivers, was repeated three times ("Prone 1", "Prone 2" and Prone 3"). The flights with stand-up and dive poses were chosen to achieve maximum and therefore most representative free fall velocities ("Stand-up 1", "Stand-up 2" and "Dive"). The purpose of the flights with rotating prone and circular motion poses was to get insight into the impact of angular motion of the GNSS antenna on the RTK performance ("Rotating Prone" and "Circular Motion"). Likewise, the flights with forward and sideward drift were intended to study the effect of lateral motion on the RTK performance ("Forward Drift" and "Sideward Drift").

The complete flight trajectory including the climb of the aircraft, the free fall phase and the parachute landing is exemplarily illustrated in Figure 8 for the first flight. The trajectory was provided by the integrated navigation system. In Figure 9, the trajectories of the free fall phase and the parachute landing of all ten flights are shown. The approach direction from the northeast to drop the skydiver was the same for all ten flights. The opening of the parachute at a height of about 1,200 metres above the ground can be clearly seen. The skydiver controlled his parachute to land in a field near the airfield's runway.

The downward velocities during the free fall phase and the parachute landing of all ten flights are plotted in Figure 10 over the height. On all flights, the skydiver quickly accelerated after jumping off the aircraft. On the flights, in which the skydiver took a prone pose (flights 1, 2, 4, 5, 7, 8, 9), the velocity curves were very similar. The skydiver reached a maximum velocity of between 215 and 230 km/h at a height of about 3,300 metres above the ground and slowly decelerated with decreasing height due to the increasing air drag caused by the increasing air density. The skydiver reached a velocity of about 190 to 210 km/h when opening the parachute at a height of about 1,200 metres above the ground. The flights with lateral motion (flights 5, 7, 9) generated additional lift forces on the skydiver's body, which resulted in slightly lower descent velocities. This applies in particular to the flight with forward drift. The maximum downward velocities were achieved on the two flights with stand-up pose (290 km/h and 310 km/h, respectively) and the flight with dive pose (385 km/h). During the latter, the skydiver had to actively decelerate before even reaching the steady-state free fall velocity, but accelerated a second time to a maximum downward velocity of 315 km/h.

By default, the post-processing navigation software was configured to calculate a pseudorange-based DGNSS navigation solution during take-off, climb and the first part of the free fall phase. During these times, the post-processing navigation software attempted to compute a differential navigation solution as long as valid measurements from the reference station were available, but automatically fell back to a stand-alone navigation solution otherwise. During the free fall, it was then actively switched from the pseudorange-based DGNSS positioning mode to the carrier phase-based RTK positioning mode at a height of 3,000 metres above the ground to initialize the RTK navigation solution and to start the fixing of the carrier phase ambiguities. Simulation studies showed that the later the switch from DGNSS to RTK positioning mode, i.e. at the lower the height, the higher the success rate of fixing the carrier-phase ambiguities and thus successfully computing an RTK navigation solution. This is because of the increasing residual differential tropospheric error with increasing height difference between the rover and reference GNSS antennas.

(a) Flight 1: Prone 1

(b) Flight 2: Prone 2

(c) Flight 3: Stand-up 1

(d) Flight 4: Rotating Prone

(e) Flight 5: Forward Drift

(f) Flight 6: Stand-up 2

(g) Flight 7: Circular Motion

(h) Flight 8: Prone 3

(i) Flight 9: Sideward Drift

(j) Flight 10: Dive

Figure 7. Ten flights with different poses: from “Prone” to “Dive”

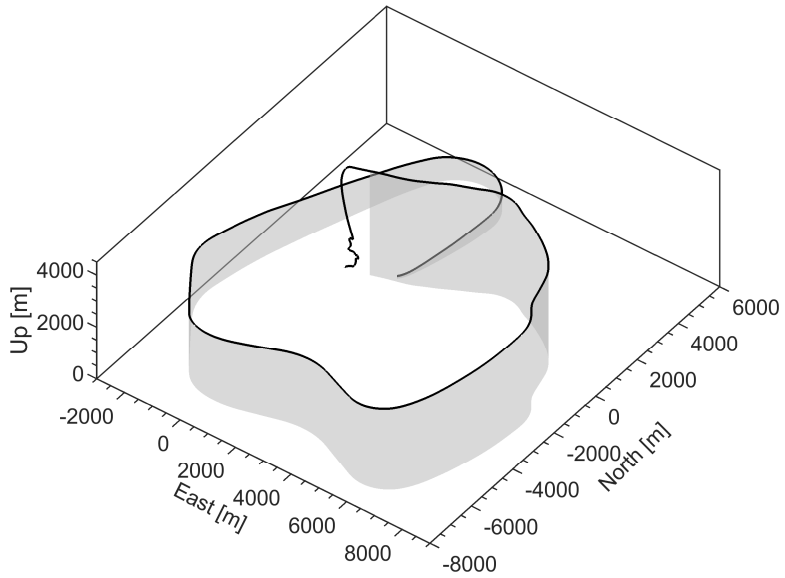

Figure 8. 3D trajectory of flight “Prone 1” from the take-off of the aircraft until parachute landing

The total number of GPS and Galileo satellites, which were used in the navigation solution by the post-processing navigation software, is shown in Figure 11 for the ten flights during the free fall phase over the height. In the free fall phase below 3,000 metres height, the GNSS measurements of nine to eighteen satellites were used in the RTK navigation solution. The number of used satellites varied more in the RTK positioning mode below 3,000 metres than in the DGNSS positioning mode above 3,000 metres above the ground because the carrier phase-based RTK navigation solution is more sensitive to signal tracking errors. As expected, the number of satellites was lowest for flight 10 because the skydiver’s head was pointing to the ground and therefore the field of view of the antenna was limited. Interestingly, the number of satellites used in the RTK navigation solution of flight 4 with the rotating prone pose was also comparably small. As will also be seen later, this is due to the phase wind-up effect that occurs when antennas slowly rotate around the boresight direction. The phase wind-up effect leads to a phase shift and hinders the successful fixing of the carrier phase ambiguities and thus the computation of an RTK navigation solution.

In Figure 12, the position differences between the navigation solutions of the rover GNSS receiver and the integrated navigation system in east, north and vertical directions are plotted over the height for the ten flights. The commanded switch from the DGNSS to the RTK positioning mode at 3,000 metres above the ground and the parachute opening at about 1,200 metres above the ground are marked by the horizontal dashed lines. The vertical blue and green coloured bar on the right side of each figure indicates whether the post-processing navigation software actually used the DGNSS positioning mode (blue) or the RTK positioning mode (green) to compute the navigation solution. For all flights except flight 10, the post-processing navigation software was able to compute an RTK navigation solution with fixed ambiguities immediately after commanding the switch from DGNSS to RTK positioning mode. Only on flight 10, it took about 140 metres of free fall until the post-processing navigation software could eventually compute an RTK navigation solution.

As expected, the position differences were much larger and noisier in the free fall phase above the switching height of 3,000 metres above the ground with a pseudorange-based DGNSS navigation solution than in the free fall phase below the switching height with a carrier phase-based RTK navigation solution. The position differences during the parachute landing phase were noisier than during the free fall phase because of the skydiver’s additional dynamics and angular motion and the shading of the parachute, both of which affect the tracking of the carrier phases of the GNSS signals. Basically, the lateral position differences in east and north directions were small on most of the ten flights during the free fall phase with an RTK navigation solution. They were in the range of some

centimetres and not biased over the height. The vertical position differences, however, were characterized by a more or less linear trend, with the position difference being maximum at the switching height and being virtually zero at zero height above the ground. The maximum vertical position differences are listed in Table 2 for the ten flights. This trend was due to the presence of the residual differential tropospheric error which was not compensated by the applied troposphere models. The residual differential tropospheric error primarily affects the vertical direction, while it largely cancels out in lateral direction due to the circumferential distributed satellites on the hemisphere. The post-processing navigation software of the rover GNSS receiver applied a different troposphere model than the post-processing navigation software of the integrated navigation system, resulting in a difference between both independent navigation solutions. The uncompensated residual tropospheric error on the double-differenced carrier phase measurements indeed falsified the position solution, but did not lead to a false fixing of the integer ambiguities, which becomes evident through the unbiased lateral position differences.
The position differences of the flights with prone pose (flights 1, 2, 8), with circular motion (flight 7) and with a small sideward drift (flight 9) were very similar and featured unbiased lateral differences and only low noise. The flights with higher downward velocities (flights 3, 6, 10) were slightly noisier but were unbiased as well in lateral direction. Only the flights with rotating prone (flight 4) and forward drift (flight 5) had partly biased lateral position errors which can actually be explained by incorrectly fixed ambiguities. The former was affected by the phase wind-up effect, and the latter by a sudden change of the satellites in view when the skydiver turned around to drift back.

Table 2: Maximum vertical position differences directly after switching from DGNSS to RTK mode

| **Flight** | 1 | 2 | 3 | 4 | 5 | 6 | 7 | 8 | 9 | 10 |
|---|---|---|---|---|---|---|---|---|---|---|
| **Vertical position difference [m]** | 0.38 | 0.37 | 0.35 | 0.81 | 0.36 | 0.26 | 0.33 | 0.39 | 0.36 | 0.29 |

## 6 CONCLUSIONS

The skydiver experiment showed that the rover GNSS receiver and the corresponding post-processing navigation software, respectively, were capable to provide an RTK navigation solution with fixed ambiguities quickly after switching from DGNSS to RTK positioning mode, even during the flight with dive pose featuring a high downward velocity. It turned out that high descent velocities do not impact the ambiguity fixing very much. In general, the residual differential tropospheric error leads to an increasing height error with increasing height difference between the reference and rover GNSS antennas which may hinder the rover GNSS receiver to fix the carrier phase ambiguities correctly and to compute an unbiased position solution. The height error of the navigation solution depends on the applied troposphere model and is mainly due to the unmodelled humidity in the air cannot be well represented by a globally valid troposphere model. Even though the residual tropospheric model resulted in vertical position differences in the range of some decimetres at 3,000 metres above the ground, RTK navigation solutions with correctly fixed ambiguities could be computed for almost all flights. However, it is advantageous that this error decreases with decreasing height above the ground because for landing RLV the high accuracy is only required close to the ground. Especially the flight with the rotating prone pose revealed that the RTK navigation solution is sensitive to the phase wind-up effect. It is therefore crucial to minimize the angular motion of the vehicle about its longitudinal axis during the landing phase or to consider the phase wind-up effect in the RTK algorithm.
In summary, the skydiver experiment proved that it is in principle possible to use RTK for accurate position estimation on landing RLV. Other aspects affecting the RTK navigation solution, like multipath, antenna phase variation, vibration and the plume of the engine, have to be considered in order to develop a robust and reliable position sensor for landing VTVL RLV.

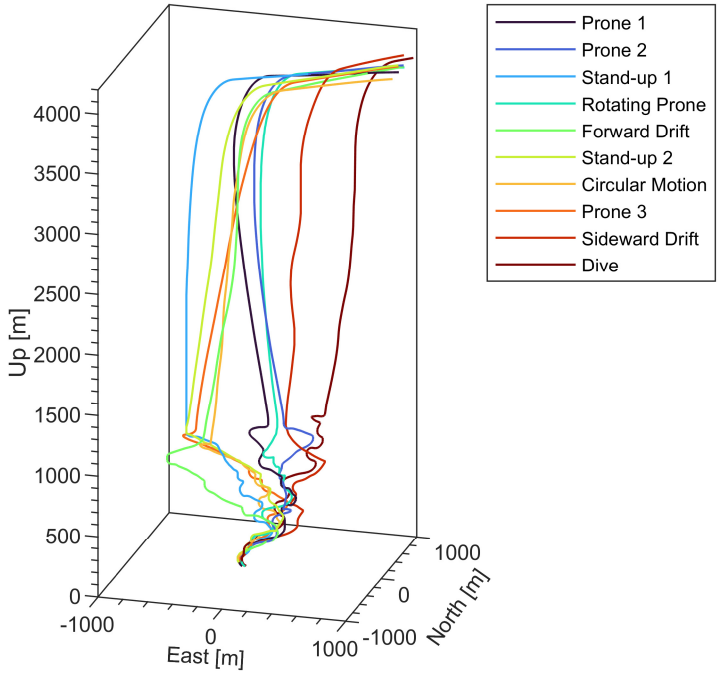


Figure 9. 3D trajectories of the free fall phase and parachute landing

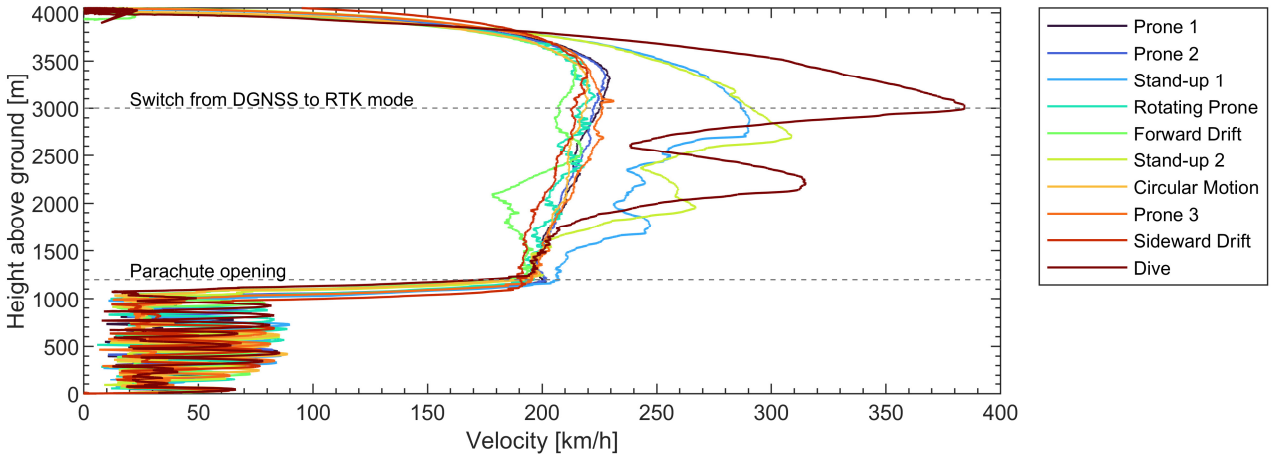


Figure 10. Downward velocities during the free fall phase and parachute landing

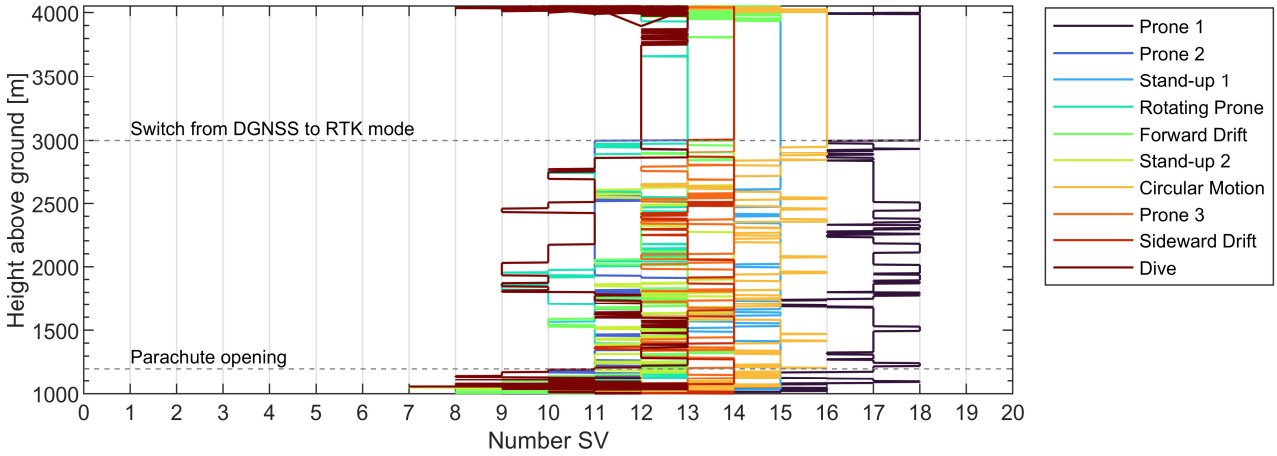


Figure 11. Number of satellites used in the navigation solution during the free fall phase

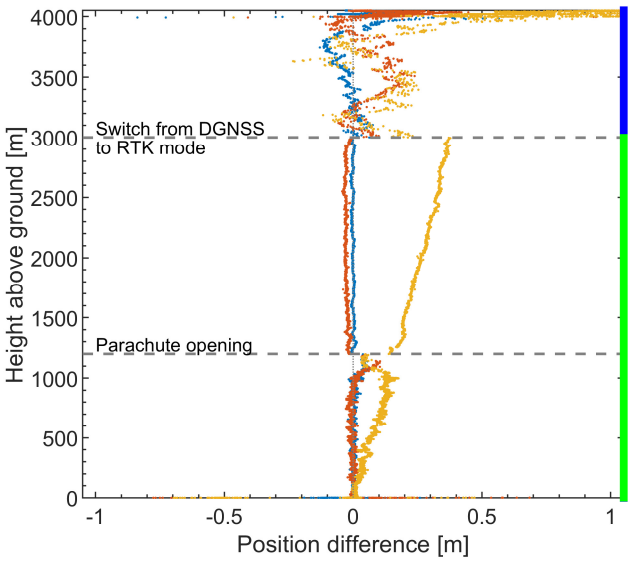


(a) Flight 1: Prone 1

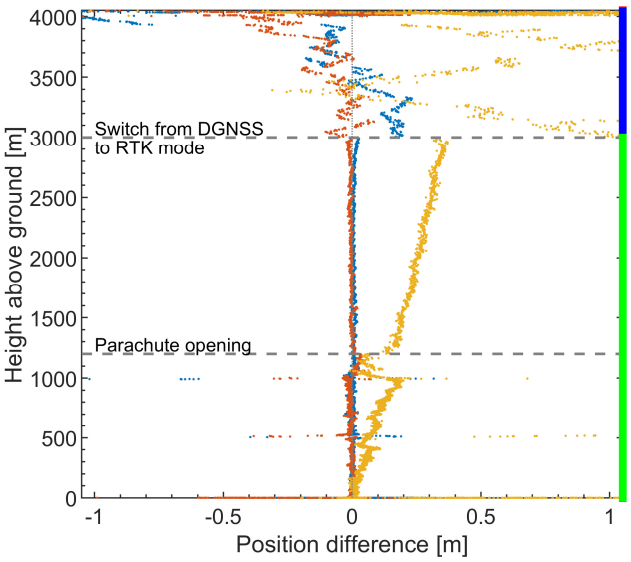


(b) Flight 2: Prone 2

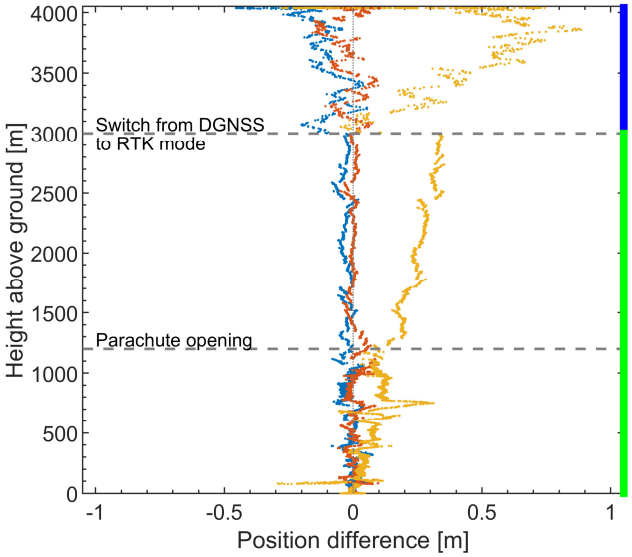


(c) Flight 3: Stand-up 1

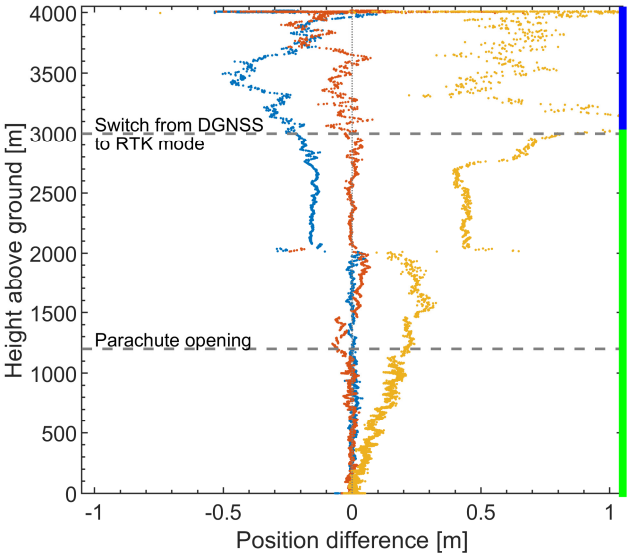


(d) Flight 4: Rotating Prone

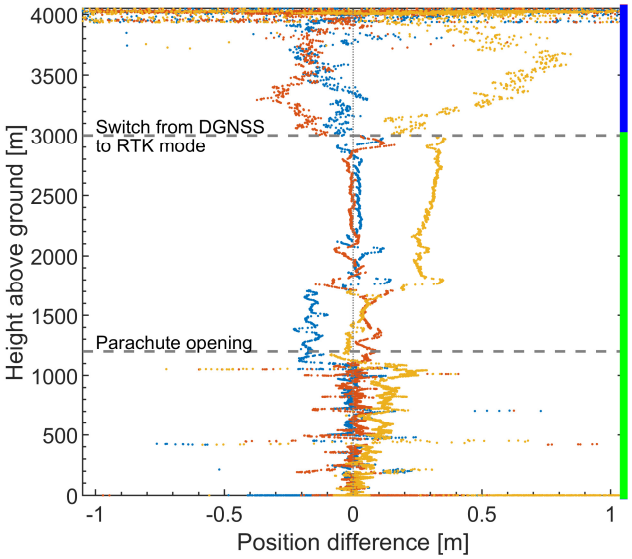


(e) Flight 5: Forward Drift

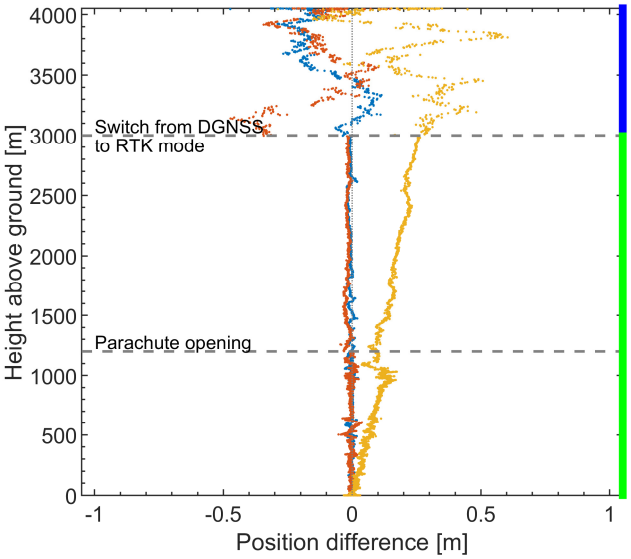


(f) Flight 6: Stand-up 2

*Figure continued on next page*

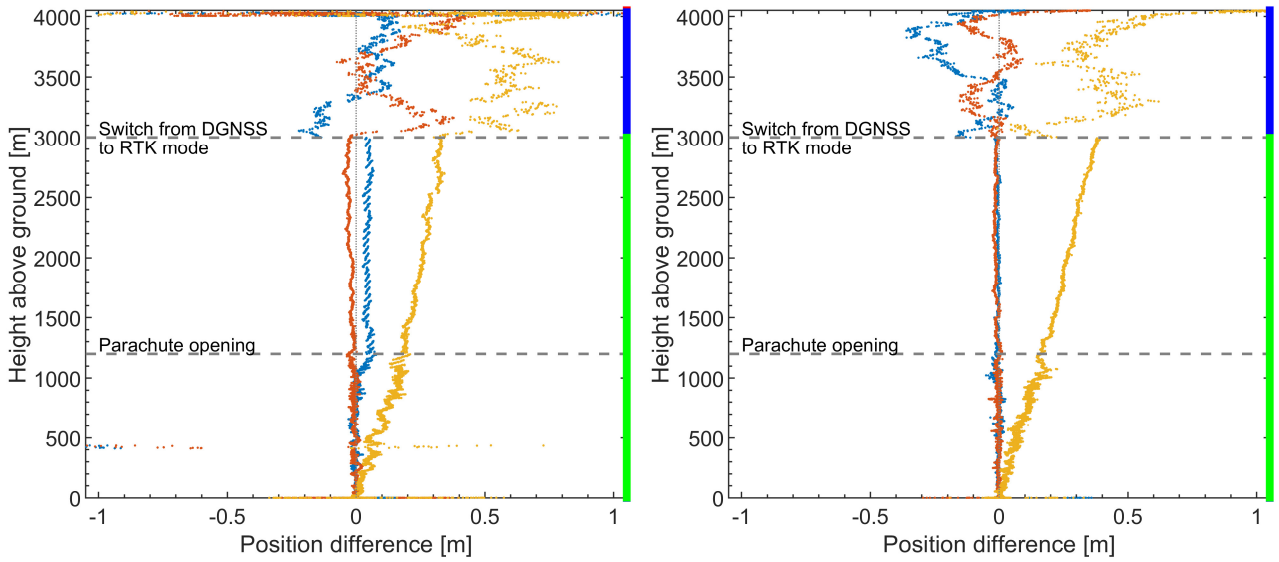


(g) Flight 7: Circular Motion




(h) Flight 8: Prone 3

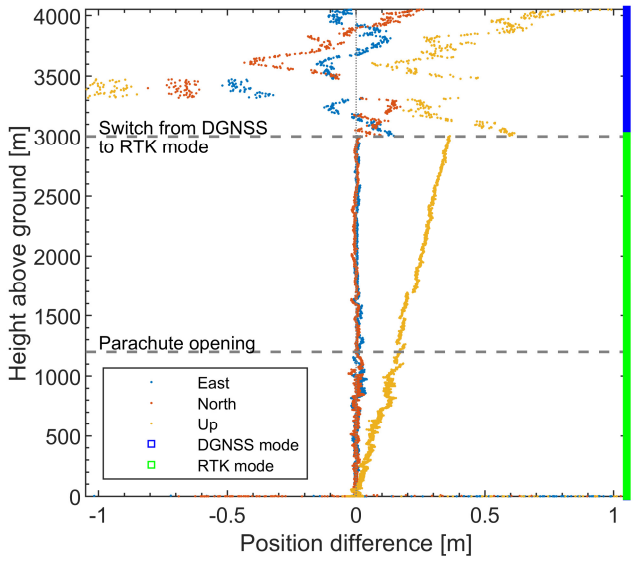


(i) Flight 9: Sideward Drift

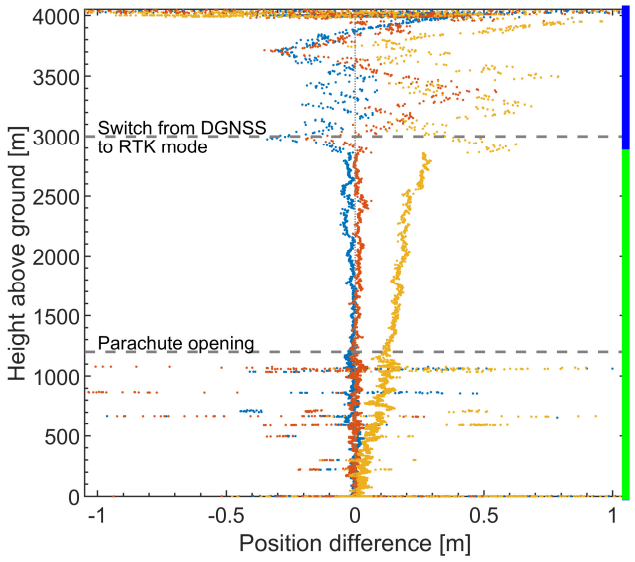


(j) Flight 10: Dive

Figure 12. Difference between the position solutions of the rover GNSS receiver and the integrated navigation system during the free fall phase and parachute landing

## 7 REFERENCES

[1] Guédron, S. et al., *CALLISTO DEMONSTRATOR: Focus on system aspects*, 71st International Astronautical Congress (IAC), 2020.

[2] Illig, M., Ishimoto, S., Dumont, E., *CALLISTO, a demonstrator for reusable launchers*, 9th European Conference for Aeronautics and Space Sciences (EUCASS), Lille, France, 2022.

[3] Dumont, E. et al., *CALLISTO: A Prototype Paving the Way for Reusable Launch Vehicles in Europe and Japan*, 73rd International Astronautical Congress (IAC), Paris, France, 2022.

[4] Schwarz, R. et al., *Preliminary Design of the Hybrid Navigation System (HNS) for the CALLISTO RLV Demonstrator*, 8th European Conference for Aeronautics and Space Sciences (EUCASS), Madrid, Spain, 2019.